Instability and confined chaos in a nonlinear dispersive wave system

Enrique A. Caponi, Philip G. Saffman,[a] and Henry C. Yuen
TRW Defense and Space Systems Group, Redondo Beach, California 90278

(Received 25 February 1981; accepted 20 July 1982)

Calculations of a discrete nonlinear dispersive wave system show that as the degree of nonlinearity increases, the system experiences in turn, periodic, recurring, chaotic, transitional, and periodic motions. A relationship between the instability of the initial configuration and the long-time behavior is identified. The calculations further suggest that the corresponding continuous system will exhibit chaotic motions and energy-sharing among a narrow band of unstable modes, a phenomenon which we call "confined chaos."

I. INTRODUCTION

There have been many recent reports of chaotic behavior in nonlinear dynamical[1] systems. In this paper, we present a series of calculations of a nonlinear dispersive wave system which is nonconservative but phase-space volume preserving. The particular example we consider corresponds to nonlinear gravity waves on deep water. Numerical solutions for initial conditions corresponding to modulated wave trains exhibit, in turn, periodic, recurring, chaotic, transitional and periodic behaviors, as the nonlinearity of the system is increased.

A relationship between the stability of the initial configuration and the long-time evolution is identified. This relationship permits one to foretell the type of behavior which will be encountered in the time evolution of a particular initial condition.

Further approximations of the governing equations lead to the well-known nonlinear Schrödinger equation, which is conservative and is derivable from a Hamiltonian. It is shown that the nonlinear Schrödinger equation also shows periodic, recurring, and chaotic behavior, but does not return to predictable behavior for strong nonlinearity, as in the case of the nonconservative system. This absence of return to predictability can also be understood in terms of the relationship between stability and evolution.

Our calculations further suggest that the evolution of nonlinear, deep-water, gravity waves exhibits "confined chaos" in a narrow band of wavenumbers.

II. GOVERNING EQUATIONS

We study the system of nonlinear ordinary differential equations

$$i\frac{dD_{\mathbf{k}_m}(t)}{dt}+\omega(\mathbf{k}_m)D_{\mathbf{k}_m}(t)=\sum_{\mathbf{k}_m+\mathbf{k}_n=\mathbf{k}_i+\mathbf{k}_j}\mathrm{T}(\mathbf{k}_m,\mathbf{k}_n,\mathbf{k}_i,\mathbf{k}_j)D^*_{\mathbf{k}_n}(t)D_{\mathbf{k}_i}(t)D_{\mathbf{k}_j}(t), \tag{1}$$

where $\mathbf{k}_m$ is a two-dimensional vector, and the frequency $\omega(\mathbf{k})$ and the interaction coefficient $\mathrm{T}(\mathbf{k}_m,\mathbf{k}_n,\mathbf{k}_i,\mathbf{k}_j)$ are real.

[a] Applied Mathematics, California Institute of Technology, Pasadena, California 91125.

This system is the discretized version of a nonlinear integro-differential equation (Zakharov equation) which governs the time evolution of spectral components in a weakly nonlinear dispersive wave system in which four-wave interactions dominate in the time scale of interest, and which is encountered in a wide range of physical phenomena including plasma physics, solid state physics, quantum field theory, and water waves.[2] We choose to consider deep-water gravity waves, for which $\omega(\mathbf{k})=(g|k|)^{1/2}$ with g being the gravitational acceleration, and T is a real interaction coefficient given in the Appendix. To leading order, the free surface displacement $\eta(\mathbf{x},t)$ is

$$\eta(\mathbf{x},t)=\sum_m\left[D_{\mathbf{k}_m}(t)\exp(i\mathbf{k}_m\cdot\mathbf{x})+D^*_{\mathbf{k}_m}(t)\exp(-i\mathbf{k}_m\cdot\mathbf{x})\right] \tag{2}$$

and the energy of displacement to this order of approximation is

$$E(t)=\sum_m|D_{\mathbf{k}_m}(t)|^2. \tag{3}$$

It can be seen that the evolution of $E(t)$ satisfies

$$\frac{dE}{dt}=-i\sum_{\mathbf{k}_m+\mathbf{k}_n=\mathbf{k}_i+\mathbf{k}_j}\left[\mathrm{T}(\mathbf{k}_m,\mathbf{k}_n,\mathbf{k}_i,\mathbf{k}_j)-\mathrm{T}(\mathbf{k}_i,\mathbf{k}_j,\mathbf{k}_m,\mathbf{k}_n)\right]\times D^*_{\mathbf{k}_m}(t)D^*_{\mathbf{k}_n}(t)D_{\mathbf{k}_i}(t)D_{\mathbf{k}_j}(t). \tag{4}$$

For our particular approximation of water wave evolution, the interaction coefficient is such that $\mathrm{T}(\mathbf{k}_m,\mathbf{k}_n,\mathbf{k}_i,\mathbf{k}_j)\neq\mathrm{T}(\mathbf{k}_i,\mathbf{k}_j,\mathbf{k}_m,\mathbf{k}_n)$ and thus $E(t)$ is not conserved by the system. Furthermore, since $\mathrm{T}(\mathbf{k}_m,\mathbf{k}_n,\mathbf{k}_i,\mathbf{k}_j)\neq\mathrm{T}(\mathbf{k}_n,\mathbf{k}_m,\mathbf{k}_i,\mathbf{k}_j)$, it follows that

$$\frac{\partial}{\partial D^*_{\mathbf{k}_m}}\left(\frac{dD_{\mathbf{k}_n}}{dt}\right)\neq\frac{\partial}{\partial D^*_{\mathbf{k}_n}}\left(\frac{dD_{\mathbf{k}_m}}{dt}\right);$$

therefore the system is not Hamiltonian with $D_{\mathbf{k}_m}$ and $D^*_{\mathbf{k}_m}$ as conjugate variables. It should be noted that the exact equations of water waves are conservative, and that a Hamiltonian exists.[3] The Zakharov equation approximation (1) is an asymptotic expression describing the slow variations of the dominant components of a wave system, and the components it retains do not conserve total energy at every instant to the order considered. There appears to be no irreversible depletion or increase of energy, however, only an aperiodic oscillation with repeated returns to the original

 0031-9171/82/122159-08$1.90

level is detected.

Comparison with experimental data indicates that the Zakharov equation is a very good approximation to deep-water gravity waves with weak to moderate nonlinearity.[4] The fact that it is a nonconservative equation approximating a conservative system should not be of concern, as the Navier–Stokes equations form a well-known nonconservative approximation to the conservative Liouville system. We also note that Eq. (1) represents a wide range of weakly nonlinear systems by different choices of T and ω, and is therefore of general interest in the study of physical problems. We can write Eq. (1) in the form $dy/dt = \mathbf{f}(\mathbf{y})$ with

$$\mathbf{y} = \begin{pmatrix} \vdots \\ D_m \\ \vdots \\ D_m^* \\ \vdots \end{pmatrix}, \qquad \mathbf{f}(\mathbf{y}) = \begin{pmatrix} \vdots \\ i\omega_m D_m - i \sum_n \sum_j T_{m,n+j-m,n,j} D^*_{n+j-m} D_n D_j \\ \vdots \\ i\omega_m D^*_m + i \sum_n \sum_j T_{m,n+j-m,n,j} D_{n+j-m} D^*_n D^*_j \\ \vdots \end{pmatrix}, \tag{5}$$

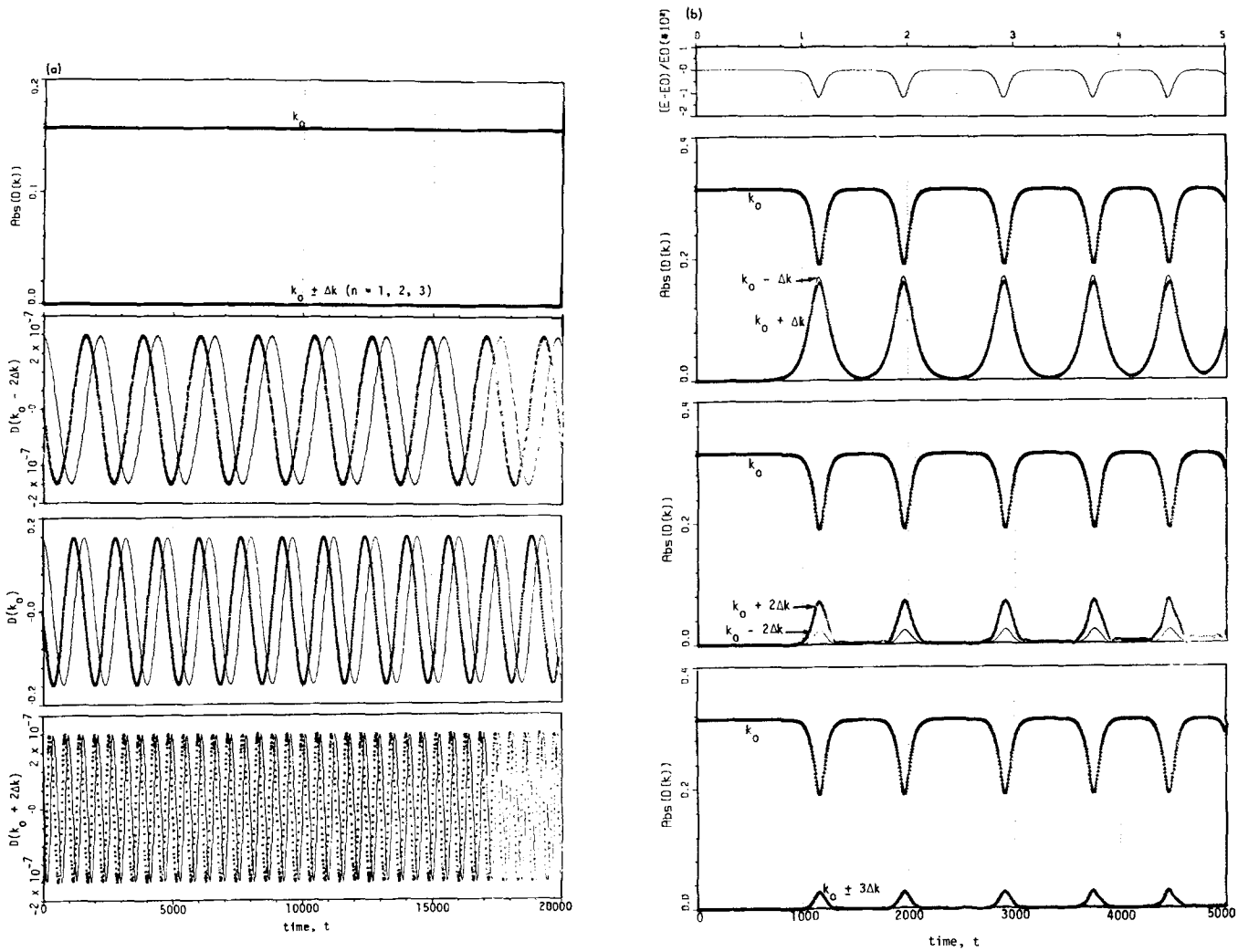

FIG. 1. (General) Effects of nonlinearity (measured by a_0) on the time evolution; (a) $a_0 = 0.05$. Top trace: Magnitudes (absolute values) of all modes. Second trace: Real (——) and imaginary parts (□□□) of $D_{k_m}(t)\exp(-i\omega_m t)$ for $k_m = k_0 - 2\Delta k$. Third trace: Real and imaginary parts of mode at k_0. Bottom trace: Real and imaginary parts of mode at $k_0 + 2\Delta k$; (b) $a_0 = 0.1$. Top trace: Total energy. Second trace: Magnitudes of modes k_0 (△△△), $k_0 - \Delta k$ (——), $k_0 + \Delta k$ (+ + +). Third trace: Magnitudes of modes k_0, $k_0 - 2\Delta k$ (——), $k_0 + 2\Delta k$ (+ + +). Fourth trace: Magnitude of modes k_0, $k_0 - 3\Delta k$ (——), $k_0 + 3\Delta k$ (+ + +); (c) $a_0 = 0.2$. Top trace: Magnitudes of modes k_0 (△△△), $k_0 - \Delta k$ (——), $k_0 + \Delta k$ (+ + +). Second trace: Magnitudes of modes k_0, $k_0 - 2\Delta k$ (——), $k_0 + 2\Delta k$ (+ + +). Third trace: Magnitude of modes k_0, $k_0 - 3\Delta k$ (——), $k_0 + 3\Delta k$ (+ + +). (d) $a_0 = 0.45$. For legend, see Fig. 1(c); (e) $a_0 = 0.5$. Magnitudes of all modes.

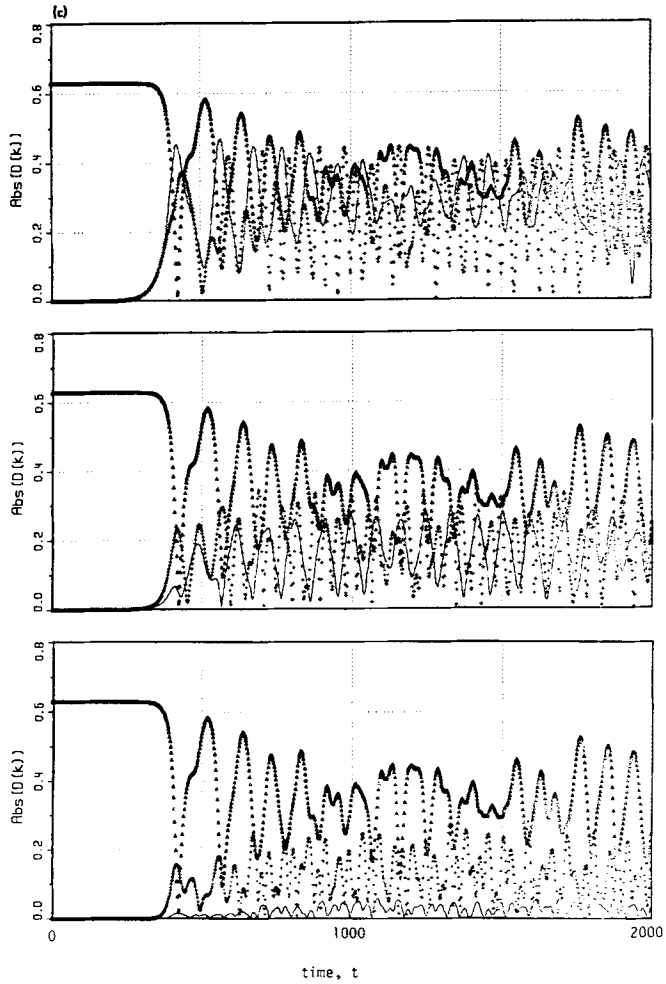

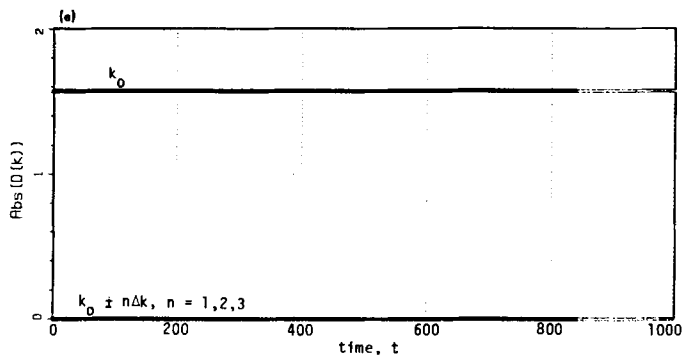

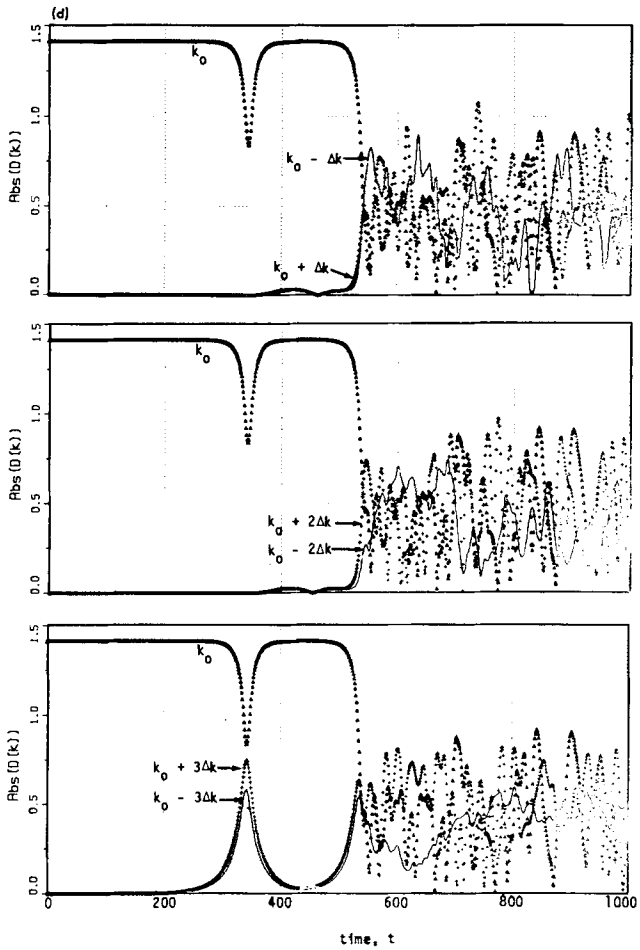

FIG. 1 (*Continued*).

where the subscripts denote dependence on various components of $\mathbf{k}$. The divergence of $\mathbf{f}$ is

$$\nabla\cdot\mathbf{f} = \sum_m \frac{\partial f_m}{\partial y_m} \equiv 0. \tag{6}$$

Hence, the system is volume-preserving in the phase space, in contrast to systems exhibiting strange attractor behavior.

Solution of the set of first-order nonlinear ordinary differential equations (5) is performed with an ODE Solver developed by the Sandia Laboratories on a PRIME 750 computer. The routine automatically interpolates at output points. The time-stepping uses a modified divided difference form of the Adams Pece formulas and local extrapolation. The routine adjusts the order and step size to control the local error per unit step in a generalized sense.

III. RESULTS

We consider unidirectional wave propagation, that is the case when $\mathbf{k}_m = (k_m, 0)$. An initial condition corresponding to a uniform wave train with wavenumber k_0 and wave amplitude a_0 is given by

$$D_m(0) = \begin{cases} \pi a_0, & \text{when } k_m = k_0, \\ 0, & \text{when } k_m \neq k_0. \end{cases} \tag{7}$$

A small perturbation in the form of a long-wave modulation

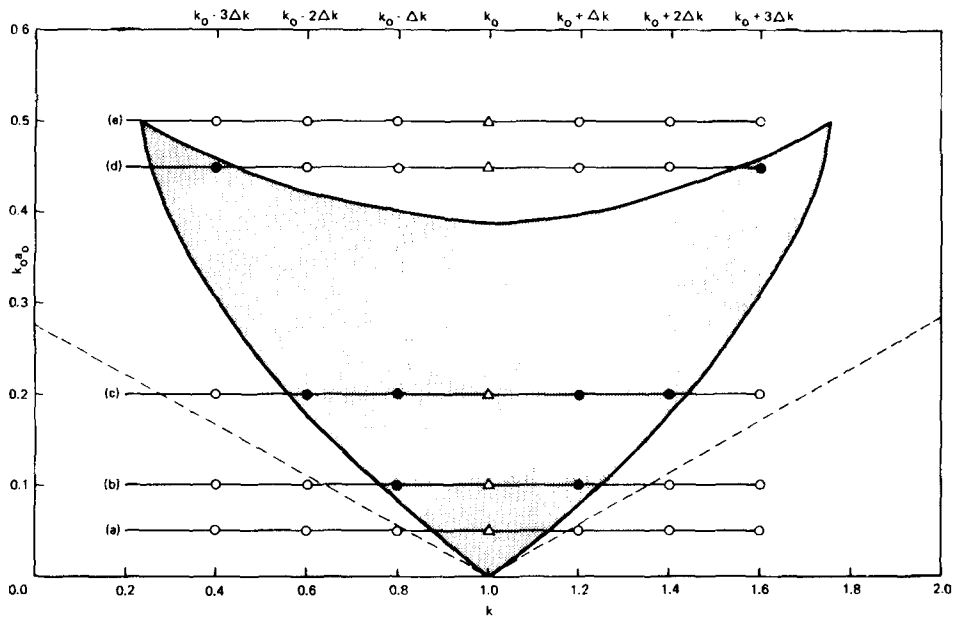

FIG. 2. Instability diagram for a uniform wave train with amplitude a_0, wavenumber k_0, subject to perturbations with wavenumber $k - k_0$. The uniperturbed system has a single mode at k_0 (denoted by Δ). The perturbations for the various cases shown in Fig. 1 are located at points labeled by ○ or ●. Solid symbols indicate unstable modes. Open symbols indicate stable modes. Dashed line is corresponding results for the nonlinear Schrödinger equation (see discussion in text).

with wavelength $2\pi/\Delta k$ is represented by the presence of nonzero components located at $k_0 \pm \Delta k$. The magnitudes of these "sidebands" correspond to the strength of the modulations, and the ratio $k_0/\Delta k$ gives the number of carrier waves in one modulation period. Confidence in a given calculation is established by comparison of results obtained using different error tolerances. For the cases exhibited, the results for error tolerances set at 10^{-8} and at 10^{-12} are not distinguish-

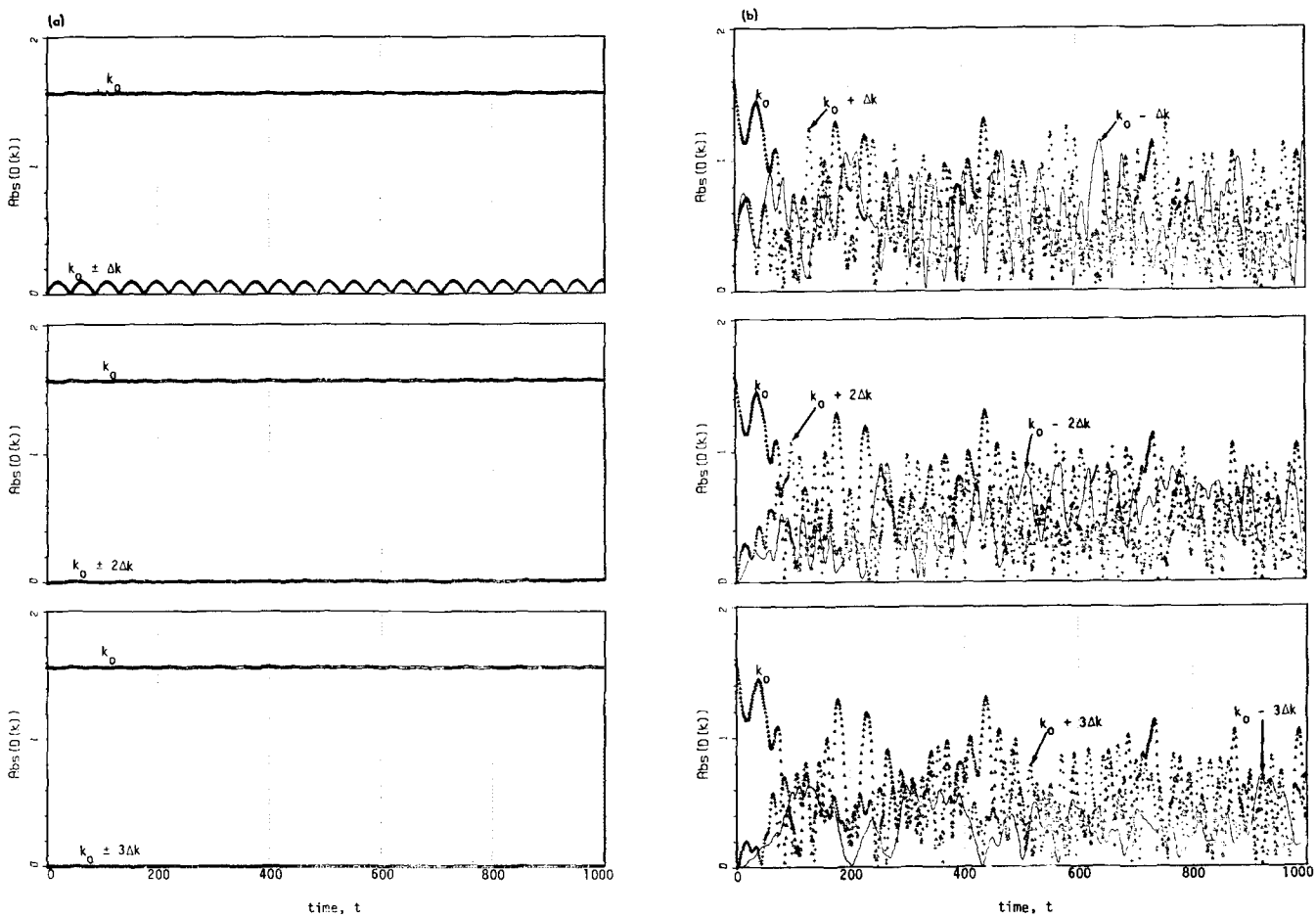

FIG. 3. Calculated time histories for a linearly-stable case with different initial modulation magnitudes: (a) $a_0 = 0.5$ with initial sideband perturbations $D(k_0 - \Delta k) = 0.01\ \pi a_0$, $D(k_0 + \Delta k) = -0.01\ i\pi a_0$. For legend, see Fig. 1(c); (b) $a_0 = 0.5$ with initial sideband perturbations $D(k_0 - \Delta k) = 0.1\ \pi a_0$, $D(k_0 + \Delta k) = -0.1\ i\pi a_0$.

able on plots within the length of records shown. As will be seen in the figures, the various types of behavior (periodic, recurring, chaotic, and transitional) are clearly established by the records; even though much longer evolutions (up to 10 times that of the records shown) were computed in most cases. There is no new information contained in the extended computations that can change our conclusions.

In all our computations, we use the normalization that $k_0 = 1$. The initial strength of the sidebands is 10^{-6} compared to the primary mode at k_0 unless otherwise specified. Results presented here have been obtained with seven modes, which is the minimum required to illustrate the phenomena of interest.

In Fig. 1, we show the results of a series of calculations with modes located at k_0, $k_{\pm 1} = k_0 \pm \Delta k$, $k_{\pm 2} = k_0 \pm 2\Delta k$, $k_{\pm 3} = k_0 \pm 3\Delta$, with $\Delta k = 0.2k_0$. The initial conditions for D_m are $D_0 = \pi a_0$, $D_m = 10^{-6}\pi a_0$ $(m = 1,2,3)$, and $D_{-m} = -10^{-6} i\pi a_0$ $(m = 1,2,3)$. In this series the wave amplitude a_0 is varied with all other parameters kept constant.

In Fig. 1(a), $a_0 = 0.05$, and the motion is periodic. The sideband components included in the calculations oscillate but their magnitudes remain small. In Fig. 1(b) $a_0 = 0.10$, and the motion is "recurring." It can be seen that the sidebands at $k_0 \pm \Delta k$ grow to a significant level (approaching the primary), and then subside, reconstructing the initial condition almost perfectly insofar as the amplitudes of the modes are concerned. The other components in the calculation receive some energy and grow and decay in phase with the sidebands at $k_0 \pm \Delta k$. The process repeats in time, although not with perfect periodicity. This behavior is normally referred to as the Fermi-Pasta Ulam recurrence, as opposed to Poincarè recurrence, which requires the return of both amplitude and phase to their initial states.[5] Note that the energy oscillates in time, but does not dissipate on the average. In Fig. 1(c), $a_0 = 0.2$, and the motion is "chaotic." By chaotic we merely mean that no apparent order can be detected in the time history. More precise definitions of chaos in terms of the behavior of the time spectrum of the system requires computational times longer than feasible. In Fig. 1(d), $a_0 = 0.45$, and the motion is first apparently recurring, but transits to chaotic behavior at a later time. Finally, in Fig. 1(e), $a_0 = 0.50$, and the system has returned to one with periodic motion.

This set of behaviors can be related to the stability properties associated with the initial conditions. The stability diagram for infinitesimal perturbations on a uniform wave train has been calculated by Crawford *et al.*[6] and is shown in Fig. 2. Superposed on the diagram are the various cases we have computed, labeled a, b, c, d, and e. It can be seen that for

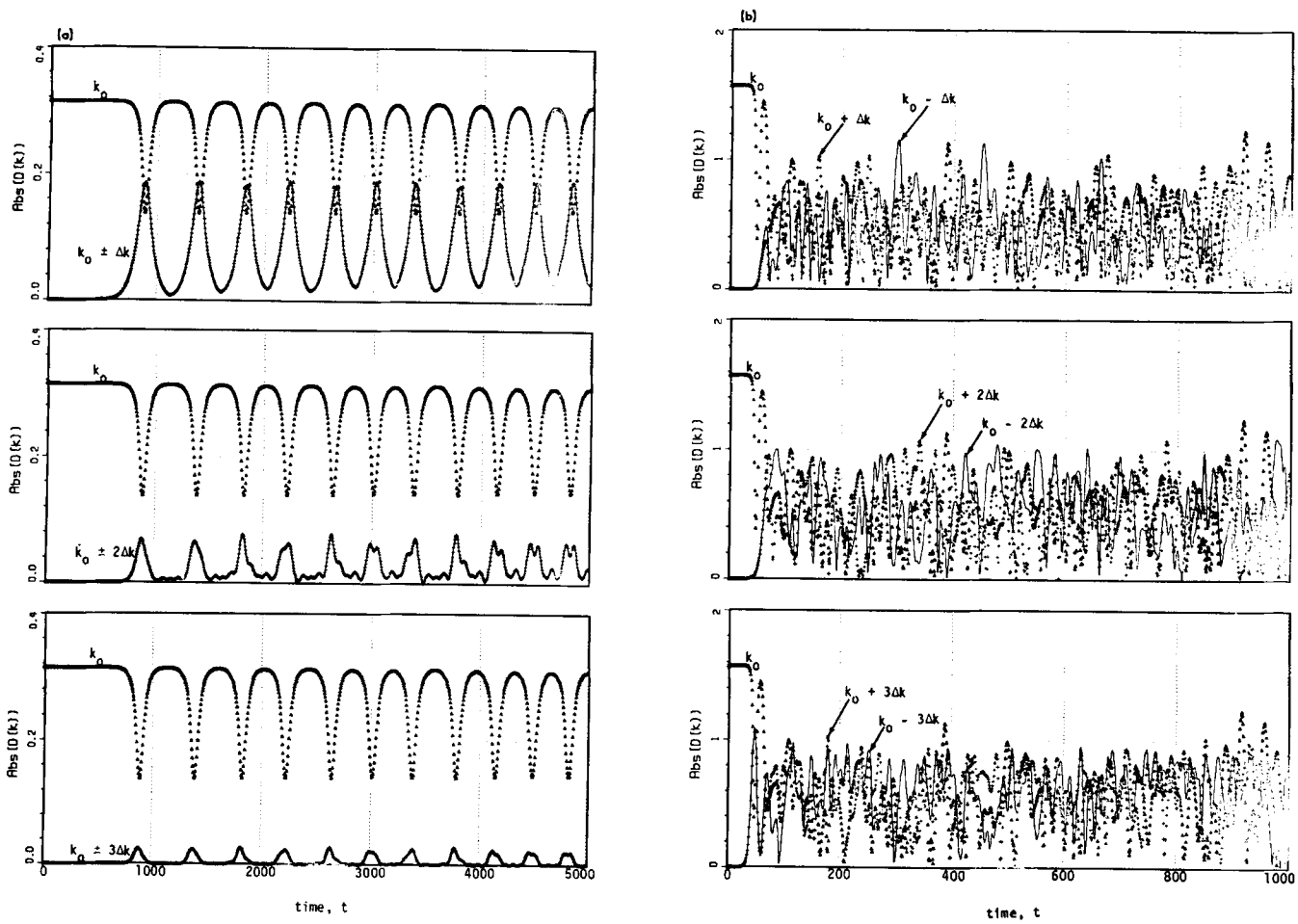

FIG. 4. Time evolution of the nonlinear Schrödinger equation approximation for $a_0 = 0.1$. For legend, see Fig. 1(c); (a) $a_0 = 0.1$. For legend, see Fig. 1(c); (b) $a_0 = 0.5$. For legend, see Fig. 1(c).

case a [corresponding to the calculation shown in Fig. 1(a)], all the included modes are stable. For case b, the sidebands at $k_0 \pm \Delta k$ are unstable, but all other components are stable. For case c, both the pairs at $k_0 \pm \Delta k$ and $k_0 \pm 2\Delta k$ are unstable. The latter pair can be interpreted as the second harmonic of the modulational perturbation, since it corresponds to modulations with wavelengths $2\pi/2\Delta k$, half of that associated with the sidebands at $k_0 \pm \Delta k$. For case d, only the outer pair of components (at $k_0 \pm 3\Delta k$) are unstable. Finally, all components are stable again for case e.

These observations indicate that periodic motion is associated with stable perturbations (cases a and e). Indeed, the oscillation frequency is predicted by the stability analysis. When only the inner set of components ($k_{\pm 1} = k_0 \pm \Delta k$) is unstable, the motion is recurring. The unstable components grow according to the instability results, return to almost their initial states and become unstable again. The other stable components behave as forced components of the unstable modes, and are more or less phase-locked to them. When more than one set of components are unstable, the motion is apparently chaotic, dominated by the nonlinear interaction of the various unstable modes. In fact, on the basis of cumulative mean values, one can detect a tendency to partition the energy of the system among the unstable components and the primary. In this sense, a partial thermalization is achieved.

Of most interest is the transitional behavior of case d. For small times, the behavior appears to be recurring involving only the primary mode at $k_0 \pm 3\Delta k$. However, for a later time, the other modes which are linearly stable participate in the energy sharing process, and a chaotic behavior follows. The involvement of these linearly stable modes (at $k_0 \pm \Delta k$ and $k_0 \pm 2\Delta k$) is caused by nonlinear instability, which is expected to be effective only when the nonlinearity of the system and the magnitude of the perturbations are sufficiently large. Unlike the linear instability the growth rate of the nonlinearly unstable mode is dependent on its own magnitude. For small times, the magnitudes of the modes was small enough not to trigger significant growth. However, these modes eventually receive energy from the linearly unstable modes at $k_0 \pm 3\Delta k$ during the recurring cycle, and nonlinear instability sets in. Chaotic beahvior then appears as a consequence of interactions among all the unstable modes.

Evidence of nonlinear instability when a_0 is large can be seen for $a_0 = 0.5$, when the system has restabilized against linear instabilities. We have computed the time evolution of initial conditions corresponding to a uniform wave train perturbed by a pair of sidebands located at $k = k_0 \pm \Delta k$ with strengths 10^{-2} and 10^{-1} that of the fundamental mode at k_0.

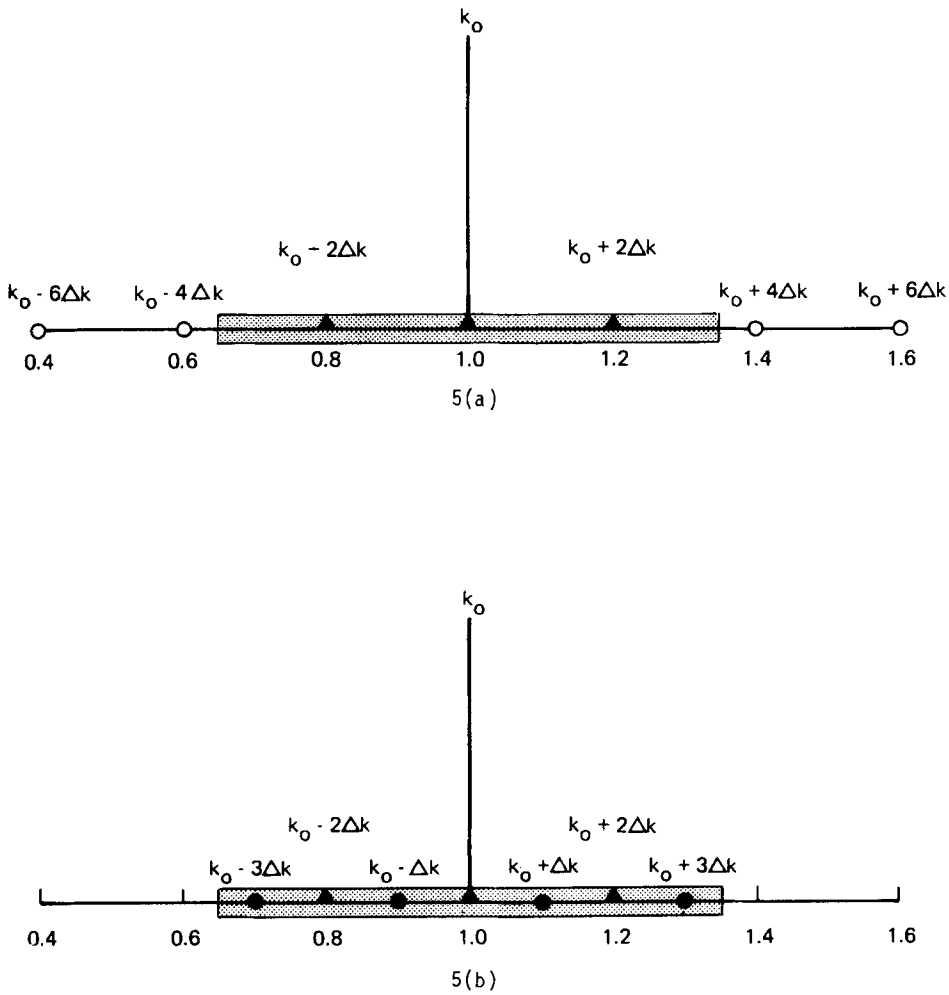

FIG. 5. Initial condition corresponding to a uniform wave train at k_0 perturbed by a 1% sideband components at $k_0 \pm 2\Delta k$, where $\Delta k = 0.1\ k_0$, for $a_0 = 0.15$: (a) Mode distribution in which only one pair of unstable modes is included. (b) Mode distribution in which all three pairs of modes included are unstable.

In Fig. 3(a), we see that sideband magnitude of $10^{-2}\ \pi a_0$ leads to a nonlinear oscillation, which is clearly nonexponential initially. In Fig. 3(b), the sideband magnitude was increased to 10^{-1}. The initial growth rate increased correspondingly by an order of magnitude. The oscillation triggers the growth of the other modes and a chaotic state results.

In the limit of weak nonlinearity and small Δk, Eq. (1) can be further approximated by taking $T(\mathbf{k}_m,\mathbf{k}_n,\mathbf{k}_i,\mathbf{k}_j)$ to be $T(\mathbf{k}_0,\mathbf{k}_0,\mathbf{k}_0,\mathbf{k}_0)$, and expanding $\omega(\mathbf{k})$ in Taylor series about $\mathbf{k}_0$ to second order. The resulting set of equations is the discretized Fourier transform of the well-known nonlinear Schrödinger equation.[2,7] As a consequence of the simplifying assumption on T, the system is now conservative and Hamiltonian in the conjugate variables D_m and D_m^*. The stability diagram for a uniform wave train subject to infinitesimal perturbations is shown in Fig. 2, where instead of the shaded region, the instability region covers all the region above the dashed lines. Consequently, we expect from the foregoing discussions to observe periodic, recurring, and then chaotic motions, but there should be no return to periodicity for large a_0. This is verified by the results shown in Fig. 4 where we presented initial conditions corresponding to cases c and e according to Fig. 2.

IV. DISCUSSION

In this paper, we have reported calculations which support a relationship between the stability of the initial condition with its subsequent evolution for a nonlinear, nonconservative, but phase-space volume preserving system. We have demonstrated that the evolution may be periodic, recurring, transitional or chaotic, depending on the initial conditions. We have shown that in a sufficiently nonlinear system, nonlinear instability must be taken into account in addition to linear instability. It is also interesting to note that for weak nonlinearity and small sideband separation, this system can be approximated by a conservative Hamiltonian system, which exhibits part, but not all, of the phenomena observed.

Another conclusion which is suggested by these results is that the calculated evolution of the wave system may depend crucially on the choice of modes included in the calculation. To illustrate this point, we show in Fig. 6 the evolution of the initial condition

$$\begin{aligned} &D(k) = \pi a_0, \quad k = k_0 \\ &D(k) = 10^{-2}\,\pi a_0, \quad k = k_0 + 2\Delta k \\ &D(k) = -i\,10^{-2}\,\pi a_0, \quad k = k_0 - 2\Delta k \\ &D(k) = 0(10^{-6}\,\pi a_0), \quad \text{all other } k \end{aligned} \tag{8}$$

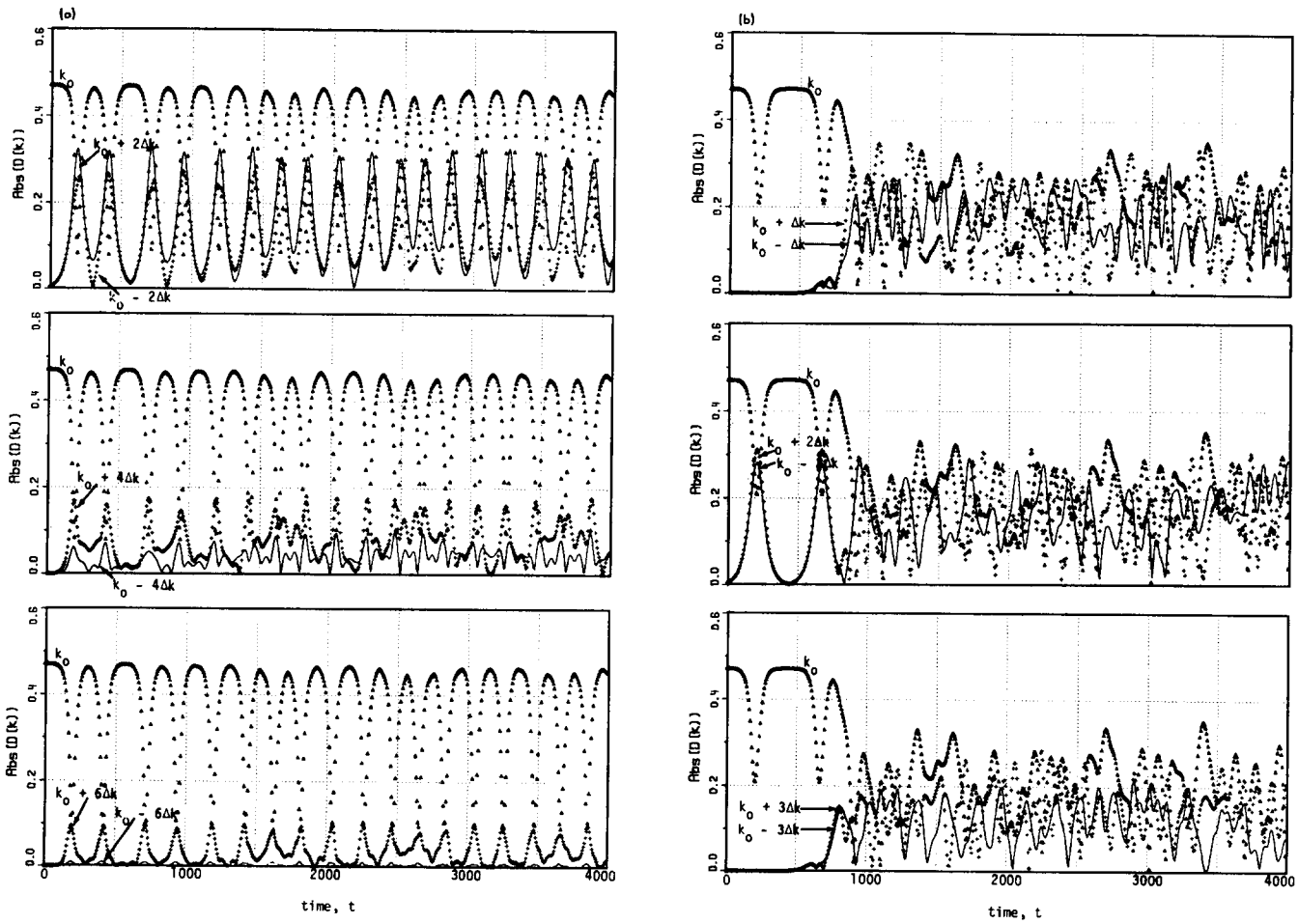

FIG. 6. Effects of mode distributin: (a) Time evolution of a uniform wave train perturbed by sideband components at $k_0 \pm 2\Delta k$ with initial condition and mode distribution given by Fig. 5(a). (b) Time evolution of a uniform wave train perturbed by sideband components at $k_0 \pm 2\Delta k$ with initial condition and mode distribution given by Fig. 5(b).

with $a_0 = 0.15$ and $\Delta k = 0.1k_0$, using two different distributions of modes (see Fig. 5). Figure 6(a) shows the results using 7 modes located at k_0, $k_0 \pm 2\Delta k$, $k_0 \pm 4\Delta k$, $k_0 \pm 6\Delta k$. With this choice, only the $k_0 \pm 2\Delta k$ pair is unstable, and the calculated behavior is "recurring." Figure 6(b) shows the results using 7 modes located at k_0, $k_0 \pm \Delta k$, $k_0 \pm 2\Delta k$, $k_0 \pm 3\Delta k$. The initial condition remains to be (8). The calculated behavior is "chaotic" in the long run, since all the modes included were unstable. Hence, calculations using only the most unstable sidebands and their harmonics (which must be stable according to results of Crawford *et al.*) which predict recurring motion[8] can be misleading, for if more unstable modes are allowed in the calculations, chaotic behavior would result. This seems to suggest that nonlinear water waves form an inherently chaotic system. However, the chaos is confined to a small range of wavenumbers which are initially unstable. We term this phenomenon confined chaos.

APPENDIX

Adopting the simplifying notation, we write $T(k,k_1,k_2,k_3) = T_{0,1,2,3}$. We have

$$T_{0,1,2,3} = 2\left(\frac{k_0\omega_1\omega_2\omega_3}{\omega_0 k_1 k_2 k_3}\right)^{1/2} T^z_{0,1,2,3}$$

with

$$\begin{aligned} T^z_{0,1,2,3} = &- \frac{2V^{(-)}_{3,3-1,1}V^{(-)}_{0,2,0-2}}{\omega_{1-3} - \omega_3 + \omega_1} \\ &- \frac{2V^{(-)}_{2,0,2-0}V^{(-)}_{1,1-3,3}}{\omega_{1-3} - \omega_1 + \omega_3} - \frac{2V^{(-)}_{2,2-1,1}V^{(-)}_{0,3,0-3}}{\omega_{1-2} - \omega_2 + \omega_1} \\ &- \frac{2V^{(-)}_{3,0,3-0}V^{(-)}_{1,1-2,2}}{\omega_{1-2} - \omega_1 + \omega_2} - \frac{2V^{(-)}_{0+1,0,1}V^{(-)}_{2+3,2,3}}{\omega_{2+3} - \omega_2 - \omega_3} \\ &- \frac{2V^{(+)}_{-2-3,2,3}V^{(+)}_{0,1,-0-1}}{\omega_{2+3} + \omega_2 + \omega_3} + W_{0,1,2,3}, \end{aligned}$$

where the second-order interaction coefficients $V^{(\pm)}_{0,1,2}$ are defined as

$$\begin{aligned} V^{(\pm)}_{0,1,2} = \frac{1}{8\pi\sqrt{2}} &\left[(\mathbf{k}_0\cdot\mathbf{k}_1 \pm k_0k_1)\left(\frac{\omega_0\omega_1}{\omega_2}\frac{k_2}{k_0k_1}\right)^{1/2}\right. \\ &+ (\mathbf{k}_0\cdot\mathbf{k}_2 \pm k_0k_2)\left(\frac{\omega_0\omega_2}{\omega_1}\frac{k_1}{k_0k_2}\right)^{1/2} \\ &\left.+ (\mathbf{k}_1\cdot\mathbf{k}_2 + k_1k_2)\left(\frac{\omega_1\omega_2}{\omega_0}\frac{k_0}{k_1k_2}\right)^{1/2}\right]. \end{aligned}$$

with $k_i = |\mathbf{k}_i|$, $\omega_i = \omega(k_i)$; and the third order interaction coefficient $W_{0,1,2,3} = W(\mathbf{k},\mathbf{k}_1,\mathbf{k}_2,\mathbf{k}_3)$ is defined as

$$\begin{aligned} W_{0,1,2,3} = &\overline{W}_{-0,-1,2,3} + \overline{W}_{2,3,-0,-1} \\ &- \overline{W}_{2,-1,-0,3} - \overline{W}_{-0,2,-1,3} \\ &- \overline{W}_{-0,3,2,-1} - \overline{W}_{3,-1,2,-0} \end{aligned}$$

with

$$\begin{aligned} \overline{W}_{0,1,2,3} = &\frac{1}{64\pi^2}\left(\frac{\omega_0\omega_1}{\omega_2\omega_3}k_0k_1k_2k_3\right)^{1/2} \\ &\times [2(k_0 + k_1) - k_{1+3} - k_{1+2} \\ &- k_{0+3} - k_{0+2}], \end{aligned}$$

and $k_{i\pm j} = |\mathbf{k}_i \pm \mathbf{k}_j|$; $\omega_{i\pm j} = \omega(k_{i\pm j})$.

[1] T. Yamada and R. Graham, Phys. Rev. Lett. **45**, 1322 (1980); P. Holmes, Philos. Trans. Roy. Soc. London **292**, 419 (1979); J. M. Greene, J. Math. Phys. **20**, 1183 (1979); *Topics in Nonlinear Dynamics: A Tribute to Sir Edward Bullard*, edited by S. Jorna (AIP Conference Proceedings No. 46 1978).

[2] V. E. Zakharov, Zh. Eksp. Teor. Fiz. **51**, 688 (1966) [Sov. Phys. JETP **24**, 455 (1967)]; V. E. Zakharov, Zh. Eksp. Teor. Fiz. **51**, 1107 (1966) [Sov. Phys. JETP **24**, 740 (1967)]; P. G. Saffman and H. C. Yuen, Phys. Rev. Lett. **44**, 1097 (1980).

[3] V. E. Zakharov, Zh. Prikl. Mekh. Tekh. Fiz. **2**, 86 (1968) [J. App. Mech. Tech. Phys. **2**, 190 (1968)].

[4] H. C. Yuen and B. M. Lake, Annu. Rev. Fluid Mech. Vol. 12, 303 (1980).

[5] E. A. Jackson, Rocky Mtn. J. Math. **8**, 127 (1978).

[6] D. R. Crawford, B. M. Lake, P. G. Saffman, and H. C. Yuen, J. Fluid Mech. **105**, 177 (1981).

[7] H. C. Yuen and W. E. Ferguson, Jr., Phys. Fluids **21**, 1275 (1978a); Phys. Fluids **21**, 2116 (1978b); D. U. Martin and H. C. Yuen, Phys. Fluids **23**, 881 (1980).

[8] B. M. Lake, H. C. Yuen, H. Rungaldier, and W. E. Ferguson, Jr., J. Fluid Mech. **83**, 49 (1977).